Chemical Science

Accepted Manuscript

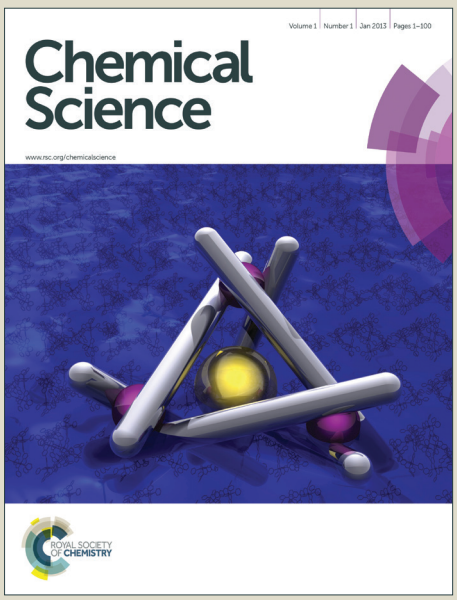

ROYAL SOCIETY OF CHEMISTRY

www.rsc.org/chemicalscience

Journal Name

RSCPublishing

ARTICLE

Arylsulfanyl Radical Lifetime in Nanostructured Silica: Dramatic Effect of the Organic Monolayer Structuration

Cite this: DOI: 10.1039/xoxxoooooox

Received ooth January 2012,
Accepted ooth January 2012

DOI: 10.1039/xoxxoooooox

www.rsc.org/

François Vibert,[a] Sylvain R. A. Marque,[a] Emily Bloch,[b] Séverine Queyroy,[a] Michèle P. Bertrand,[a]* Stéphane Gastaldi,[a]* Eric Besson[a]*

Nanostructured hybrid silicas in which covalently anchored aromatic thiols are regularly distributed over the pore enable a dramatic increase in the half-lifetimes of the corresponding arylsulfanyl radicals. This enhancement is not only due to limited diffusion but also to the structuration of the organic monolayer on the surface of the pores. Molecular dynamics modeling shows that at high loadings, in spite of their spatial vicinity, supramolecular interactions disfavor the coupling of arylsulfanyl radicals. As compared to phenylsulfanyl radical in solution, the half-lifetime measured at 293 K can be improved up by 9 orders of magnitude to reach 65 h.

Development of new materials with unusual functional groups, like transient radicals, is of topical interest to enable new advances in spin sciences. The notions of transience, persistence and stability of radical species are not widespread amongst the chemical community. Radicals can be classified depending on their lifetime. According to Ingold, a radical can be transient (half-life < 10^{-3} s), persistent (half-life > 10^{-3} s) or even stable (storable in air).[1,2] Therefore, increasing the half-lifetime of a radical species from a microsecond to a tenth of second can be considered as making persistent a transient radical. Most radicals are highly reactive and transient in nature. The propensity of unpaired electrons to pair up with one another to form closed-shell molecules is responsible for the high rate constants of radical/radical reactions and of most radical/molecule reactions.[3] However, many radicals such as for instance triphenylmethyl, phenalenyl, hydrazyl, nitroxyl or thioaminyl radicals transgress this behavior.[4] These radicals can be tailored to become extremely persistent or even stable through the subtle interplay of steric and/or electronic effects.

Stable open shell molecules are useful tools. They are extensively applied in electron paramagnetic resonance (EPR) spectroscopy techniques like spin trapping,[5,6,7,8] spin labeling[9] or EPR imaging.[10] Other properties related to the presence of unpaired electrons such as conductivity or magnetism have been studied in order to develop smart devices.[11,12] Further progress in spin sciences, based on stable neutral radicals, can be expected from the design and synthesis of stable neutral radicals with novel molecular and electronic structures.[13] In this context, the development of a versatile approach enabling to transform a transient radical to a highly persistent or stable one without changing its structural features remains a challenging task. This can lead to the discovery of new properties of radical species which cannot be explored at present due to their rapid decay.

Organic radicals and materials have already a long common history as evidenced by the pioneering studies performed at low temperature in the sixties.[14] More recently, organic radical precursors have been adsorbed in zeolites.[15,16,17,18,19] Extensive studies of the influence of supramolecular binding with zeolites on the recombination of benzylic radicals have been reported by Turro, who correlated the rate of radical decay to steric effects in internal supercages. Organic radical precursors have also been grafted onto silica[20] and nanostructured silicas.[21,22,23] The increase of radical lifetimes,[15,20] as well as the modification of their reactivity,[21] were rationalized in term of limited diffusion and/or interactions with the surface. It must be underlined that in all these studies the organic radical precursor was introduced in the material by simple adsorption or by post-grafting, in other words with no means to control the distribution of the radical precursor in the inorganic material.

We report herein a versatile approach to increase the persistence of radicals by the simultaneous control of the diffusion and the close environment of the radical species, and not by the modification of steric or electronic factors. To reach this goal, radical precursors must be accurately located in an inorganic matrix, designed to prevent termination reactions. The direct synthesis of organic-inorganic hybrid nanostructured materials, by the use of the Sol-Gel process in the presence of structure-directing agents, enables functional nanostructured silicas in which the radical precursors are regularly distributed in the pores to be engineered.[24] This approach offers the possibility to investigate the incidence of the structuration of the hybrid material on the radical lifetime and, as a consequence, to correlate the persistence to parameters such as loading, nature of the spacer, and presence of residual silanols on the pore surface.

Results and discussion

To implement such an approach, a model radical, showing a broad range of reactivity in solution, was selected. Arylsulfanyl radicals were considered good models since they are reactive species involved in hydrogen atom abstraction, addition to π systems or dimerization reactions.[25,26,27] They are by nature transient as illustrated by their diffusion-controlled recombination rate.[28] They can be easily generated by photolysis of the corresponding thiophenols.

Although arylsulfanyl radicals are transient species, they have been extensively studied and characterized by a large number of spectroscopic methods such as EPR or laser flash photolysis.[26,29] The EPR signal of phenylsulfanyl radical was detected in organic glasses.[26,30] From flash photolysis, its half-lifetime was estimated about 200 µs at room temperature.[31] We experimented that a signal could only be observed below 153 K under irradiation of a thiophenol benzene glass. Moreover, when the same experiment was reproduced with thiophenol adsorbed on non-functionalized SBA-15 silica, the spectrum of sulfanyl radical was observed below 173 K and no persistence was noted. There is no effect of the nanostructured environment on the phenylsulfanyl radical lifetime.

Besides the ease to generate radicals from UV-transparent hybrid silicas by simple photolysis, the use of an arylthiol as a radical precursor leads to several advantages that will be discussed below.

Triethoxysilane derivatives **1** and **2** were selected as radical precursors (Scheme 1). The thiol group was protected as a thioester in order to avoid the formation of disulfides during the synthesis of the hybrid material. The hydrolysis of the thioester groups during the sol-gel process generated thiol functions, which led to anchored arylsulfanyl radicals upon UV irradiation. The main difference between **1** and **2** lies in the chemical nature of the spacer connecting the aromatic ring to the surface of the silica, i.e., urea and ether, respectively. Assuming a fully extended molecule, the distance between silicon and sulfur atoms in the most stable conformation was estimated (B3LYP/6-31+G(d, p)) at 1.36 and 1.11 nm for the thiophenols corresponding to **1** and **2**, respectively.

The first step in our approach consisted in the preparation of a series of periodic mesoporous hybrid silicas in which the radical precursors were covalently linked to silicon atoms and localized inside the pores. 2D hexagonal SBA type silicas were prepared by co-condensation of alkyltriethoxysilane **1** or **2** and tetraethyl orthosilicate (TEOS) in the presence of P123 ($PEO_{20}PPO_{70}PEO_{20}$) as structure directing agent. The resulting materials were named **SBA$_n$-1** in which **1** specifies the nature of the organic precursor and n indicates the TEOS/radical precursor molar ratio determined after the characterization of the hybrid silicas. The use of the Sol-Gel process in the presence of structure-directing agents induces a regular distribution of the organic radical precursor. The average distance between organic chains was estimated from standard analyses (Table 1).

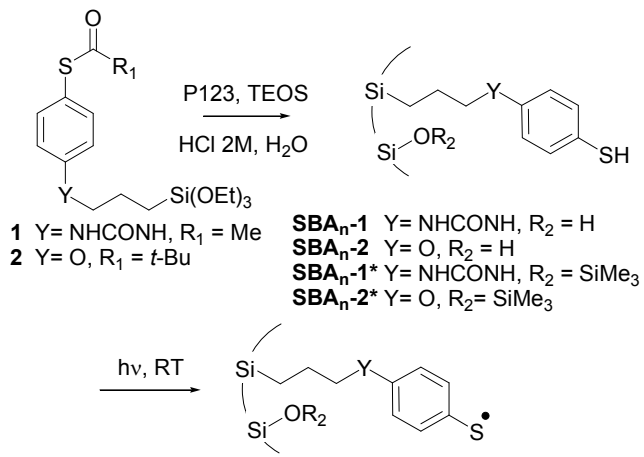

Scheme 1. Synthesis and photolysis of radical precursors localized in the pores of the silica

As mentioned above, deacetylation of precursors **1** and **2** occurred during the synthesis of the hybrid silicas. This was confirmed by the disappearance of the thioester carbonyl signal in ^{13}C CP-MAS NMR spectra at 194.6 and 200.3 ppm for **1** and **2**, respectively.

The behavior of arylsulfanyl radicals generated from precursors regularly anchored inside the pores of the silicas was studied by EPR. In a typical procedure, the functionalized material was degassed (10^{-5} mbar) in a 4 mm quartz-glass tube and arylsulfanyl radicals were generated via the photolytic cleavage of the S-H bonds inside the spectrometer cavity (xenon lamp (200-800 nm)) (Scheme 1).

An anisotropic signal, resulting from the immobilization of the precursors on the surface of the pores, was recorded whatever the hybrid silica and the loading. The EPR parameters of these signals were in agreement with the formation of arylsulfanyl radicals [32,33,34] for which the *g* tensor is axisymmetrical and the spin density is localized on the sulfur atom.[35,36] Representative spectra are shown in Figure 1.

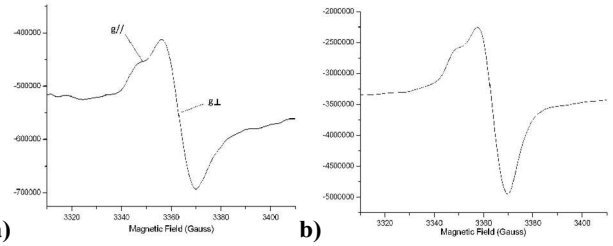

Figure 1. EPR spectra at 293K for the irradiation of **SBA$_{33}$-1** (a) and **SBA$_{37}$-2** (b)

The radical lifetimes are collected in Table 1. For both **SBA$_n$-1** and **SBA$_n$-2**, measured g_{iso} [37] ranged from 2.0081 to 2.0099.

It must be underlined that whatever the structure of the organic linker, **SBA$_n$-1** or **SBA$_n$-2**, a low intensity signal corresponding to arylsulfanyl radicals was observed before irradiation. It might result from the homolysis of a small amount of precursor under daylight. In all experiments, the irradiation was

maintained until the signal reached a quasi-stationary maximum intensity, at which point, the UV lamp was switched-off. The half-lifetimes of the anchored arylsulfanyl radicals were measured after turning off the irradiation by monitoring the decay of the signal intensity (determined from the double integrated EPR signal). The decay curves were fitted with exponential or multi-exponential models, which did not allow to determine the mechanism involved. Several termination processes occurred. The half-lifetimes were graphically estimated from the decay curves.

A dramatic increase in the lifetime compared to the value reported for phenylsulfanyl radical in solution, i.e. 200 µs,[31] was recorded in each case.

Table 1. Half-lifetime and Landé *g*-factors of arylsulfanyl radicals generated by photolysis of **SBA$_n$-1** and **SBA$_n$-2**

Entry		$g_{//}$	$g_{\perp}$	g_{iso}[a]	d[b]	$t_{1/2}$ (h)[c]
a	**SBA$_{17}$-1**	2.0141	2.0066	2.0091	1.2	> 62.4
b	**SBA$_{33}$-1**	2.0143	2.0050	2.0081	1.6	>15.0
c	**SBA$_{71}$-1**	2.0155	2.0051	2.0086	4.6	> 3.6
d	**SBA$_{239}$-1**	2.0146	2.0060	2.0089	19.6	> 18.0
e	**SBA$_{21}$-2**	2.0142	2.0077	2.0099	0.9	nd[d]
f	**SBA$_{37}$-2**	2.0142	2.0057	2.0085	1.9	9.5
g	**SBA$_{73}$-2**	2.0150	2.0054	2.0086	4.8	3.2

[a] $g_{iso} = (2g_{\perp} + g_{//})/3$. [b] Statistical average distance between organic precursors in nm. [c] Determined from the double integrated EPR signal at 293K. [d] Not determined.

- Concerning the half-lifetime ($t_{1/2}$) of the radicals issued from irradiation of **SBA$_n$-1**, the highest value, i.e. more than 62.4 h, was recorded for the highest concentration of organic precursor, i.e. **SBA$_{17}$-1**. One then observed a decrease in lifetime with loading. Half-lifetimes superior to 15 h and 3.6 h were registered for **SBA$_{33}$-1** and **SBA$_{71}$-1,** respectively. In the case of the highest dilution, **SBA$_{239}$-1**, $t_{1/2}$ exceeded 18.0 h.

- Regarding the material with the oxygenated linker, an intense EPR signal was recorded for **SBA$_{21}$-2** prior to irradiation. The increase of the signal was weak under irradiation as well as its decrease after the end of the photolysis. This phenomenon might be due to the interference of spontaneous or photo-stimulated electron transfer reactions.[38] Even though this signal indicated the presence of a persistent radical species, it was difficult to determine its half-lifetime. For lower loadings, **SBA$_{37}$-2** and **SBA$_{73}$-2**, the measured $t_{1/2}$ were 9.5 and 3.2 h, respectively.

In order to determine the effect of the surface residual silanol groups on the behavior of the radicals, the hybrid silicas were passivated upon reaction with $ClSiMe_3$ (Scheme 1). Photolytic EPR experiments were repeated with these new hybrid materials, **SBA$_n$-1*** and **SBA$_n$-2*** (Table 2).

Once again, except for **SBA$_{17}$-1***, a huge improvement of $t_{1/2}$ was observed compared to phenylsulfanyl radical in solution and the passivation accentuated this enhancement. This passivation increased the half-lifetime by 48.6 h for **SBA$_{33}$-1*** as compared to the corresponding non-passivated materials. A half-lifetime superior to 63.6 h was recorded for **SBA$_{33}$-1***. The passivation reduced the difference observed between **SBA$_{17}$-1** and **SBA$_{33}$-1**. The half-lifetime was more than 2 times higher for **SBA$_{71}$-1*** than for **SBA$_{71}$-1**. The same passivation effect was also noted with **SBA$_{37}$-2*** and **SBA$_{73}$-2*** where the half-lifetime reached 62.9 and 3.8 h, respectively. Because of its dramatic increase, $t_{1/2}$ was not measured in the case of **SBA$_{21}$-2***; the signal lost only 32% of its intensity over 80 h. In other words, the half-lifetime was by far the highest of all the series. In the case of **SBA$_{17}$-1***, the limited effect of the passivation might be explained by the low number of silanols available to the passivation due to the loading.

Table 2. Half-lifetime and Landé *g*-factors of arylsulfanyl radicals generated by photolysis of **SBA$_n$-1*** and **SBA$_n$-2***

Entry		$g_{//}$	$g_{\perp}$	g_{iso}[a]	$t_{1/2}$ (h)[b]
a	**SBA$_{17}$-1***	2.0141	2.0053	2.0082	> 65.0
b	**SBA$_{33}$-1***	2.0149	2.0038	2.0075	> 63.6
c	**SBA$_{71}$-1***	2.0145	2.0043	2.0077	8.2
d	**SBA$_{239}$-1***	2.0139	2.0056	2.0084	16.4
e	**SBA$_{21}$-2***	2.0136	2.0078	2.0097	nd[c]
f	**SBA$_{37}$-2***	2.0141	2.0079	2.0100	62.9
g	**SBA$_{73}$-2***	2.0141	2.0061	2.0088	3.8

[a] $g_{iso} = (2g_{\perp} + g_{//})/3$. [b] Determined from the double integrated EPR signal at 293K. [c] loss of 32% of signal intensity in 80 h.

In such a system, the two main processes, by which arylsulfanyl radicals can evolve, are dimerization and inter-chain hydrogen atom transfer (HAT). A significant interest in selecting thiols as radical precursors is that the degenerate HAT from a S-H group to a sulfur-centered radical does not contribute to the disappearance of arylsulfanyl radicals.

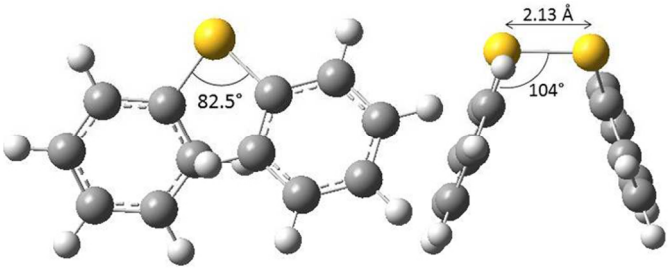

Figure 2. Favored conformation of diphenyldisulfide (B3LYP/6-311+G(d,p) level of theory)

As the spin density is mainly localized on the sulfur atom, recombination forming disulfides is the most likely cause of the decay of the arylsulfanyl radical signals.[35] MP2 calculations show that, in the cases of 4-methoxy or 4-methylureido phenylsulfanyl radical, 85% of the spin density lies on the sulfur atom. Amazingly, the data collected in tables 1 and 2 showed that the closer the organic precursors, the higher the radical lifetimes. This behavior is contra-intuitive since one would have expected that the closer the radicals are, the easier their dimerization should be, resulting in shorter lifetimes.

There is formally no activation energy for the coupling of two freely diffusing phenylsulfanyl radicals. Calculations did not allow the location of a transition structure.[39] Disulfides are known to adopt a preferential skew conformation.[40] Experimentally, a 85° dihedral angle has been measured for

crystalline diphenyl disulfides.[41,42,43] This value is coherent with our own calculation at B3LYP/6-311+G(d,p) level, which predict a 82.5° dihedral angle (CSSC), a 104° (CSS) valence angle and a 2.13 Å S-S bond length (Figure 2), and with MP2 calculations,[36] which predict a dihedral angle of 80°. This conformation enables the repulsion between the sulfur lone pairs to be minimal. The conformer is stabilized by the hyperconjugative interactions between the lone pair on one sulfur atom and the antibonding $\sigma_{S\text{-}C}$* orbital on the other sulfur atom which increase the bond order of the S-S bond. The stability and the reactivity of the S-S bridge depend on the mechanical forces exerted by its environment.[44,45] Disulfur bridges can undergo spontaneous and reversible cleavage. The biradical character of the S-S bond increases upon stretching.[46,47] It is well known that torsional strain also plays a key role: compressing the dihedral angle down to 0° enhances the 4 electron-destabilization. The resulting increase of the potential energy is amplified by 1,4-steric repulsions in the *cis* conformation.

On the basis of these data and assuming that the formation of the disulfide linkage could only be envisaged between two spatially close arylsulfanyl radicals, we have investigated the behavior of organic moieties in the pore of the silica by applying classical molecular dynamics to the modeling of an isolated functionalized pore. This simulation method is neither able to study the coupling reaction nor its reversal. However, its capacity to model large size systems leads to interesting conformational analyses. The model cylinders of silica (inner diameter 5 nm, length 6.4 nm) were built according to Brodka approach[48] and randomly functionalized with the arylsulfanyl radicals (CH_2-CH_2-CH_2-O-C_6H_4-$S^\bullet$) derived from **2**. Three virtual hybrid silicas were prepared with average inter-chain distances of 0.56, 1.10 and 1.75 nm, and were named **vSBA$_A$-2**, **vSBA$_B$-2** and **vSBA$_C$-2**, respectively. These systems were simulated under two different force fields in order to exclude any bias in the results due to the choice of one parameters set.

Modeling put into perspective the size of the pore in comparison with that of the organic precursors (Figure 3 a, c and e). The following interpretation of the data is based on the reasonable assumption that, in such a system, an arylsulfanyl radical can mainly disappear by coupling with another radical in close vicinity. In addition, the disulfide linkage should be formed in a stable conformation with minimal external mechanical stress.[44]

A striking difference was noticed between the three systems (Figure 3 b, d and f). In the case of a high loading (**vSBA$_A$-2**), due to the high density of organic moieties, aromatic rings are aligned and sulfur atoms are directed towards the center of the pore.

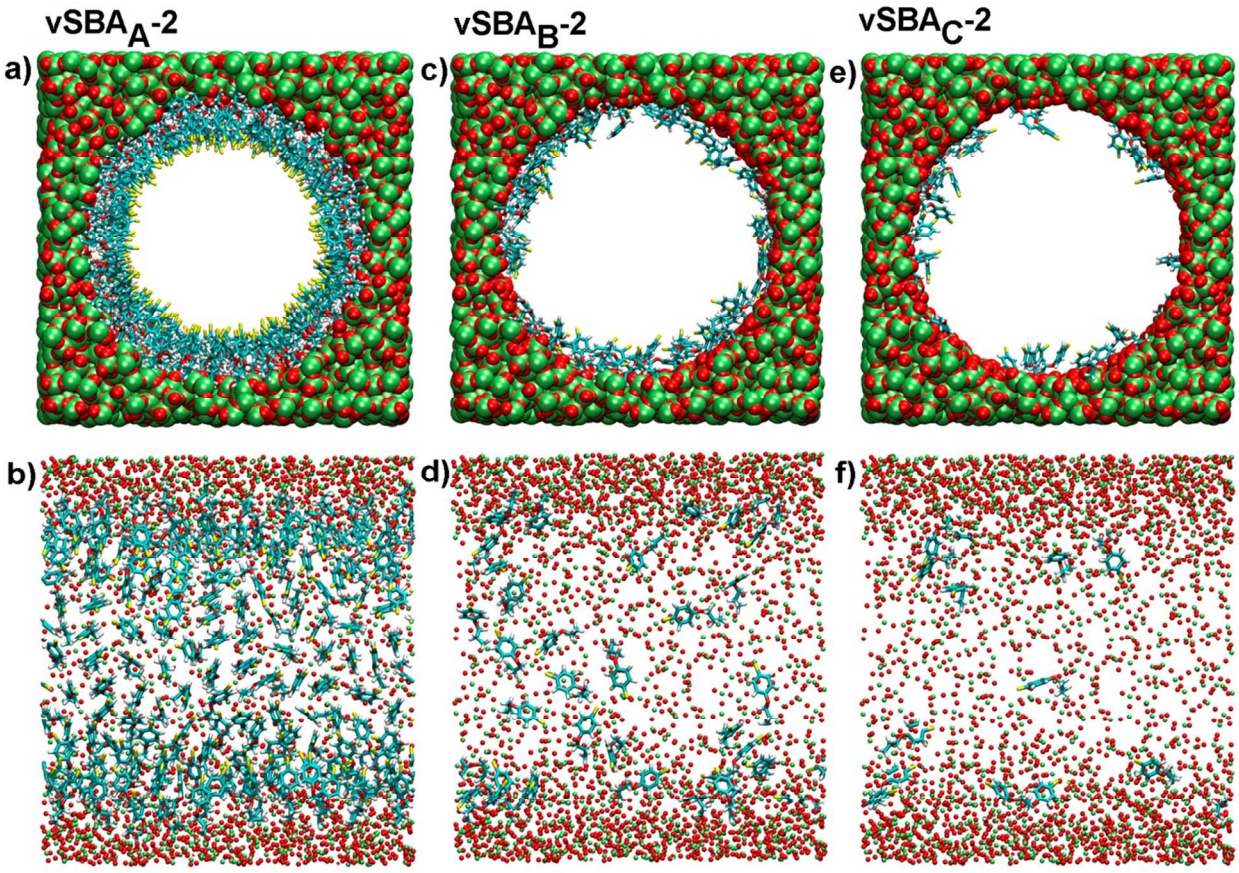

Figure 3. Snapshots of virtual silicas pores calculated with DREIDING FF: transverse section (a, c and e) and longitudinal section (b, d and f). Color key: S (yellow), C (blue), H (white), O (red), Si (green).

Conversely, with lower organic loadings, **vSBA$_B$-2** and **vSBA$_C$-2**, the behavior of organic fragments changes completely as they frequently refold over the surface. The inter-chain interactions decrease and the interactions with the surface of the silica increase.

Statistics can be extracted from these simulations. Whatever the force field, DREIDING or GAFF, the sulfur atoms are, as expected, closer to each other in higher loaded materials. The curves have the same profile with both force fields. For the sake of simplification, only the DREIDING curves are presented. (Figure 4a).

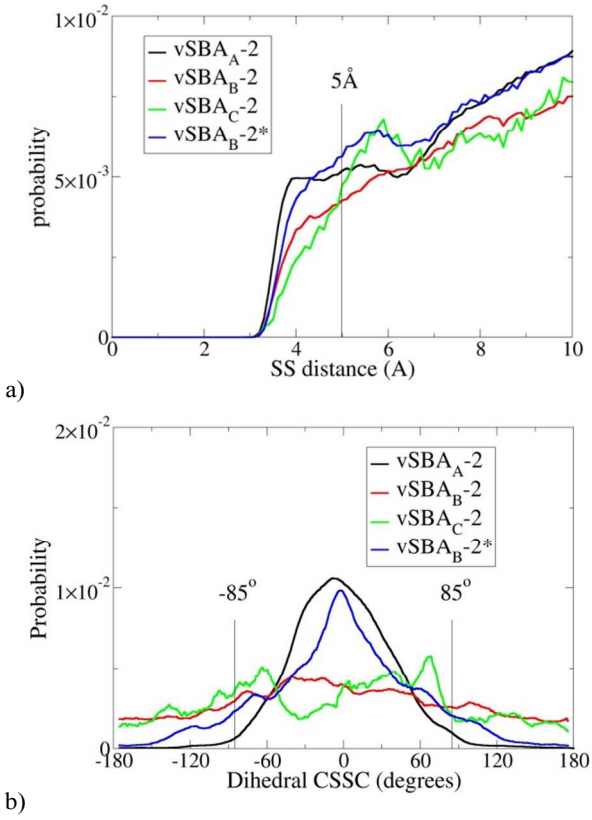

Figure 4. Distance between sulfur atoms (a) and (CSSC) dihedral angle with d(S-S)< 5 Å (b) estimated with DREIDING FF.

As already mentioned, the formation of a disulfide bond can only occur if the two sulfur atoms are reasonably close by. Therefore in the following discussion, only the cases where the inter-sulfur distance is lower than 5 Å are considered. The second parameter of interest is the dihedral angle (CSSC) (Figure 4b).

With **vSBA$_B$-2** and **vSBA$_C$-2**, the dihedral angle can reach a wide range of values, there is no constraint to dimerization. The situation is clearly different for **vSBA$_A$-2**. Most of the organic moieties have a CSSC dihedral angle close to 0° which is consistent with aligned aromatic rings directed towards the central axis of the cylinder. This average value does not fit the skew conformation, where the dihedral angle is close to 85°, which is known to be the most stable both experimentally[41,42,43] and theoretically.[36,49,50,51] Any disulfide linkage formed in such a compressed *cis* conformation would be highly energetic, as stated above. In other words, under this monolayer-like structuration the formation of disulfide is hindered. The chain flexibility is locked by steric effects with little influence of the sulfur end group. This kind of packing would similarly occur with thiols instead of sulfanyl radicals at the end of the anchored chains. Therefore, the lack of spin-coupling interactions in the force fields tested is not harmful for this analysis.

These calculations fit quite well the variation of the lifetime recorded for the radicals resulting from **SBA$_n$-1** and **SBA$_n$-2**. The lifetime decreases with the loading down to a minimum and then re-increases at high dilution in organic precursor (Table 1). In the case of **SBA$_{17}$-1** and **SBA$_{21}$-2**, the precursors form a compact layer on the surface of the pore. With such a spatial arrangement, the formation of the S-S bond in a stable conformation is made difficult because the stereoelectronic factors are unfavorable. As a consequence, an impressive half-lifetime is observed. At higher dilution, the chain length and the inter-chain distance (Table 1, entries b and f) become compatible with the coupling of two arylsulfanyl radicals. The spacing between the organic chains increases which favors their mobility and facilitates the formation of disulfide bridges as stable conformers. It must be stressed that at very high dilution (**SBA$_{239}$-1**), the organic moieties are statistically isolated, they cannot interact with each other, this results in an increase of $t_{1/2}$. The formation of the disulfide bond is unlikely. Unidentified reactions with the surface occurred as complex decay curves are observed.

The effects of passivation were also investigated by molecular dynamics. **vSBA$_B$-2** was virtually passivated to lead to **vSBA$_B$-2***. Because of the similarity between the results obtained from the previous simulations with two different force fields, only the DREIDING force field was used in this case. These calculations show that passivation precludes the refolding of the organic chain on the surface of the pore (Figure 5).

Owing to the steric hindrance of the trimethylsilyl groups, the chains that are found refolded in **vSBA$_B$-2** are forced to align in **vSBA$_B$-2*** with the sulfur atom pointing toward the center of the pore.

Statistics showed that the behavior of **vSBA$_B$-2*** becomes close to that of **vSBA$_A$-2** (Figure 4). The blue line depicting the distribution of S-S inter-distances for **vSBA$_B$-2*** can almost be superimposed on that of **vSBA$_A$-2** for distances lower than 5 Å. As regard to the CSSC dihedral angle, the effect of passivation is very important since the distribution of the values is now centered on 0°, the profile is the same as in the case of **vSBA$_A$-2**.

The passivation has a direct impact on the structuration of the organic monolayer whatever the loading. At high loadings, such as **SBA$_{17}$-1*** and **SBA$_{21}$-2***, the introduction of a trimethylsilyl group on the residual silanol groups reduces the mobility of the organic chains, as a consequence, higher $t_{1/2}$ are recorded. With intermediate loadings, as it is the case for **SBA$_{33}$-1*** and **SBA$_{37}$-2***, the improvement of the half-lifetime is even more pronounced. This can be again rationalized by a lower mobility

of the chains parted by the presence of trimethylsilyl groups. The bulky trimethylsilyl groups anchored around the organic chains reduce the length of the flexible part of the organic chains, thus with shorter flexible chains the dimerization is disfavored. The same rationale applies to lower loadings of organic groups such as **SBA$_{71}$-1*** and **SBA$_{73}$-2***.

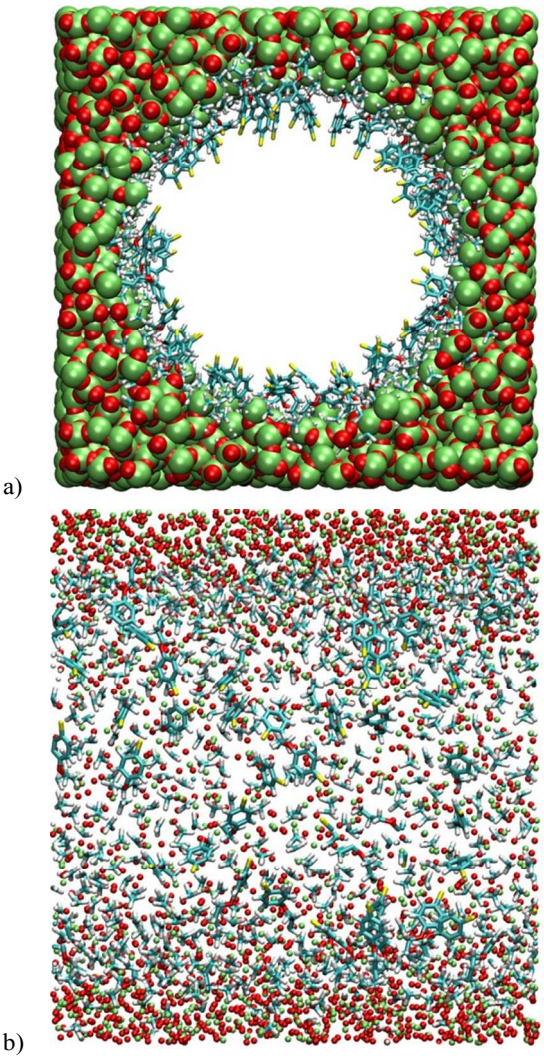

Figure 5. Snapshots of **vSBA$_B$-2*** pore calculated with DREIDING FF a) Transverse section. b) Longitudinal section. Color key: S (yellow), C (blue), H (white), O (red), Si (green).

The structuration of the organic monolayer must have an impact on the shape of the EPR spectra. The line width is a good indicator to probe the radical environment, as it is influenced by the mobility of the radical and its interactions with other radicals.

Line width values and their variations between the beginning and the end of the irradiation are gathered in Table 3 for **SBA$_n$-2** and **SBA$_n$-2*** (see supporting information for **SBA$_n$-1** and **SBA$_n$-1***).

Table 3. Variation of EPR line width for **SBA$_n$-2** and **SBA$_n$-2***

Entry		Line width		ΔH_{pp}
		H_{pp1} (G)[a]	H_{pp2} (G)[b]	
a	**SBA$_{21}$-2**	10.91	12.70	1.79
b	**SBA$_{37}$-2**	12.92	12.34	-0.58
c	**SBA$_{73}$-2**	11.96	11.67	-0.29
d	**SBA$_{21}$-2***	8.81	9.06	0.25
e	**SBA$_{37}$-2***	9.61	14.36	4.75
f	**SBA$_{73}$-2***	9.84	14.34	4.50

[a] Line width at the beginning of the irradiation. [b] Line width at the end of the irradiation (+/- 0.3G).

Line width broadening is the result of three main effects acting together: chemical exchange (conformational changes, tumbling), spin-spin exchange, and dipole-dipole interaction.[52] In the case of the low loadings (Table 3, entries b, c vs entries e, f), the line width at the beginning of the irradiation, that is at low radical concentration, is broader for non passivated silicas than for passivated ones. Due to the low radical concentration, spin-spin exchange and dipole-dipole interaction can be disregarded. This observation indicates that, in non-passivated silicas, organic fragments are less mobile due to their refolding on the surface. This experimental evidence highlights the passivation effect, which prevents the interactions between the silanol groups and the organic chains and thus the refolding on the surface. The line width increases regularly during the irradiation when the silicas are passivated as the concentration in sulfanyl radicals increases due to radical interactions.

For the non-passivated series, no significant increases were observed for **SBA$_{37}$-2** and **SBA$_{73}$-2** meaning that the interactions surface – sulfanyl radicals (chemical exchange) predominated over the spin-spin exchange and dipole-dipole interaction.

For **SBA$_{21}$-2***, the line width is nearly the same at the end of irradiation than at beginning and it increases after 80h (32% decay, Hpp=13.32G) (Figure 6). The initial single symmetric line (a), observed for strong coupling, evolved toward a broader anisotropic signal (b) with weaker exchange interactions.

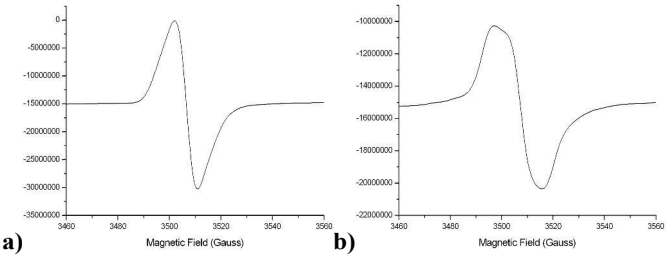

Figure 6. EPR spectra at 293K of **SBA$_{21}$-2*** at the end of the irradiation (Hpp =9.06G) (a) and after 80h (Hpp =13.32G) (b)

It is generally admitted that the line width tends to increase linearly with the concentration, due to dipolar interactions. For large enough concentration, exchange effects become appreciable and at high concentration the exchange interaction causes the line to narrow.[53] Figure 6 shows the evolution of the signal shape from the highest concentration (a), where spin

exchange is predominant, to a lower concentration, where dipolar interactions take over.
The density of radicals in **SBA_{21}-2** is large enough for spin-spin exchange or dipole-dipole interaction to occur and induce line broadening.

Conclusions

Room temperature photolysis of covalently linked aromatic thiols, regularly spread over the pores of nanostructured silicas, led to arylsulfanyl radicals with half-lifetimes which can be more than 9 orders of magnitude higher than the lifetime of phenylsulfanyl radical in solution taken as reference. Contra-intuitively, the higher the density of organic chains on the surface of the pore, the higher the lifetime. Molecular dynamics simulations showed that this huge increase is not only related to the effect of anchoring but also to the monolayer structuration of the organic precursors. At high loadings, supramolecular interactions prevent the signal decay as the dimerization of sulfanyl radicals would lead to unstable conformers of the expected disulfides with mechanical stress disfavoring the process. The passivation of residual silanols on the surface of the pore accentuates the slowing down of the radical decay. The radicals centers are spaced apart due to the restricted freedom of motion of the anchoring chains. Increasing the persistence of a radical classified as transient to such a level opens up routes to paramagnetic materials unexplored to date. This versatile approach using confinement effects is likely to be suitable for extension to other types of transient radical species.

Acknowledgements

The authors thank Dr P. Llewellyn for critical reading of the manuscript. The authors acknowledge the Agence Nationale de la Recherche for funding (ANR-12-JS07-0005). This work was supported by the computing facilities of the CRCMM, Centre Régional de Compétences en Modélisation Moléculaire de Marseille.

Notes and references

[a] Aix-Marseille Université, CNRS, Institut de Chimie Radicalaire UMR 7273, 13397 Cedex 20, Marseille, France.
E-mail : stephane.gastaldi@univ-amu.fr, eric.besson@univ-amu.fr

[b] Aix-Marseille Université, CNRS, MADIREL UMR 7246, 13397 Cedex 20, Marseille, France

Electronic Supplementary Information (ESI) available: Experimental procedures and characterizations for the organic compounds and the derived materials (NMR, TEM, SAXS, Nitrogen adsorption/desorption analysis, ATG). EPR decay curves, Variation of EPR line width for **SBA_n-1** and **SBA_n-1***, Spin density calculations, DFT calculations and molecular dynamics simulations. See DOI: 10.1039/b000000x/

[1] D. Griller and K. U. Ingold, *Acc. Chem. Res.*, 1976, **9**, 13.
[2] D. Griller and K. U. Ingold, *Acc. Chem. Res.*, 1980, **13**, 193.
[3] M. Newcomb, in *Encyclopedia of Radicals in Chemistry, Biology and Materials*, ed., C. Chatgilialoglu and A. Studer, Wiley, 2012, vol.1, ch. 5, pp 107–124.
[4] R. G. Hicks, *Org. Biomol. Chem.*, 2007, **5**, 1321.
[5] M. J. Perkins, *Adv. Phys. Org. Chem.*, 1980, **17**, 1.
[6] D. Rehorek, *Chem. Soc. Rev.*, 1991, **20**, 341.
[7] A. L. J. Beckwith, V.W. Bowry and K. U. Ingold, *J. Am. Chem. Soc.*, 1992, **114**, 4983.
[8] V. W. Bowry and K. U. Ingold, *J. Am. Chem. Soc.*, 1992, **114**, 4992.
[9] *Stable Radicals*, ed., R. G. Hicks, Wiley, 2010.
[10] J. L. Zweier and P. Kuppusamy, *Proc. Natl. Acad. Sci. U. S. A.*, 1988, **85**, 5703.
[11] I. Ratera and J. Veciana, *Chem. Soc. Rev.*, 2012, **41**, 303.
[12] N. Domingo, E. Bellido and D. Ruiz-Molina, *Chem. Soc. Rev.*, 2012, **41**, 258.
[13] M. Mas-Torrent, N. Crivillers, C. Rovira and J. Veciana, *Chem. Rev.*, 2012, **112**, 2506.
[14] N. T. Kartel, *Theor. Exp. Chem.*, 1980, **16**, 128 and references therein.
[15] N. J. Turro, *Acc. Chem. Res.*, 2000, **33**, 637.
[16] N. J. Turro, X.-G. Lei, S. Jockusch, L. Wei, Z. Liu, L. Abrams and M. F. Ottaviani, *J. Org. Chem.*, 2002, **67**, 2606.
[17] N. J. Turro and S. Jockusch, *J. Org. Chem.*, 2002, **67**, 5779.
[18] A. Moscatelli, Z. Liu, X. Lei, J. Dyer, L. Abrams, M. F. Ottaviani and N. J. Turro, *J. Am. Chem Soc.*, 2008, **130**, 11344.
[19] J. P. Da Dilva, S. Jockusch, J. M. G. Martinho, M. F. Ottaviani and N. J. Turro, *Org. Lett.*, 2012, **12**, 3062.
[20] S. Panagiota, M. Louloudi and Y. Deligiannakis, *Chem. Phys. Lett.*, 2009, **472**, 85.
[21] M. K. Kidder, P. F. Britt, Z. Zhang, S. Dai, E. W. Hagaman and A. C. Buchanan, III, *J. Am. Chem Soc.*, 2005, **127**, 6353.
[22] M. K. Kidder, P. F. Britt, A. L. Chaffee and A. C. Buchanan, III, *Chem. Commun.*, 2007, 52.
[23] M. K. Kidder, A. L. Chaffee, M.-H. T. Nguyen and A. C. Buchanan, III, *J. Org. Chem.*, 2011, **76**, 6014.
[24] C. T. Kresge and W. J. Roth, *Chem. Soc. Rev.*, 2013, **42**, 3663.
[25] M. P. Bertrand and C. Ferreri, in *Radical in Organic Synthesis*, ed., P. Renaud and M. Sibi, Wiley-VCH, Weinheim, 2001, vol. 2, pp 485–503
[26] C. Chatgilialoglu, M. P. Bertrand and C. Ferreri, in *S-Centered Radicals*, ed., Z. B. Alfassi, Wiley, Chichester, 1999, pp 311–354.
[27] F. Dénès, M. Pichowicz, G. Povie and P. Renaud, *Chem. Rev.*, 2014, **114**, 2587.

[28] T. W. Scott and S. N. Liu, *J. Phys. Chem.*, 1989, **93**, 1393.
[29] K.-D. Asmus and M. Bonifacic, in *S-Centered Radicals*, ed., Z. B. Alfassi, Wiley, Chichester, 1999, pp 141–191.
[30] Y.V. Razskazovskii and M.Y. Mel'nikov, in *S-Centered Radicals*, ed., Z. B. Alfassi, Wiley, Chichester, 1999, pp 225–244.
[31] F. C. Thyrion, *J. Phys. Chem.*, 1973, **77**, 1478.
[32] J. C. Walton, in *Encyclopedia of Radicals in Chemistry, Biology and Materials*, ed., C. Chatgilialoglu and A. Studer, Wiley, 2012, vol.1, ch. 7, 151–174.
[33] U. Schmidt, *Angew. Chem., Int. Ed.*, 1964, **3**, 602.
[34] W. Rundel and K. Scheffler, *Angew. Chem., Int. Ed.*, 1965, **4**, 243.
[35] U. Schmidt and A. Müller, *Angew. Chem., Int. Ed.*, 1963, **2**, 216.
[36] G. N. R. Tripathi, Q. Sun, D. A. Armstrong, D. M. Chipman and R. H. Schuler, *J. Phys. Chem.*, 1992, **96**, 5344.
[37] F. Gerson and Huber, W. in *Electron Spin Resonance Spectroscopy of Organic Radicals*, ed., F. Gerson and W. Huber, Wiley-VCH, 2003, pp 97–165.
[38] N. A. Borisevich, V. I. Buganov, V. L. Dobovskii, S. A. Tikhomirov and G. B. Tolstorozhev, *Optics and Spectrocopy*, 2005, **98**, 368.
[39] A. G. Vandeputte, M.-F. Reyniers and G. B. Marin, *J. Phys. Chem. A*, 2010, **114**, 10531.
[40] a) R. Benassi, G. L. Fiandri and F. A Taddei, *J. Mol. Struct.*, 1997, **418**, l27. b) L.-F. Zou, K. Shen, Y. Fu and Q.-X. Guo, *J. Phys. Org. Chem.*, 2007, **20**, 754.
[41] M. Sacerdoti and G. Gilli, *Acta Cryst.*, 1975, **B31**, 327.
[42] T. Shimizu, H. Isonon, M. Yasui, F. Iwasaki and N. Kamigata, *Org. let.*, 2001, **3**, 3639.
[43] T. Schaefer, S. R. Salman, T. A. Wildman and P. D. Clark, *Can. J. Chem.*, 1982, **60**, 342.
[44] I. B. Baldus and F. Gräter, *Biophys. J.*, 2012, **102**, 622.
[45] N. L. Haworth, J. Y. Liu, S. W. Fan, J. E. Gready and M. A. Wouters, *Austr. J. Chem.*, 2010, **63**, 379.
[46] E. Dumont, J.-F. Loos and X. Assfeld, *Chem. Phys. Lett.*, 2008, **458**, 276.
[47] M. F. Iozzi, T. Helgaker and E. Uggerud, *J. Phys. Chem A*, 2011, **115**, 2308.
[48] A. Brodka and T. W. Zerda, *J. Chem. Phys.*, 1996, **104**, 6319.
[49] D. Nori-Shargh, H. Yahyaei and J. E. Boggs, *J. Mol. Graphics Modell.* 2010, **28**, 807.
[50] R. S. Sengar, V. N. Nemykin and P. Basu, *New J. Chem.*, 2003, **27**, 1115.
[51] N. L. Haworth, J. Y. Liu, S. W. Fan, J. E. Gready and M. A. Wouters, Aust. J. Chem., 2010, **63**, 379.
[52] a) *Electron Paramagnetic Resonance*, ed., J. A. Weil and J. R. Bolton, John Wiley & Sons, 2007. b) *Principles of Electron Spin Resonance*, ed., N. M. Atherton, Ellis Horwood, 1993.
[53] K. M. Salikhov, *Appl. Magn. Reson.*, 2010, **38**, 237.

